

Electronic Supplementary Information

Mesoporous “Shell-in-Shell” Structured Nanocatalyst with Large Surface Area, Enhanced Synergy, and Improved Catalytic Selectivity for Suzuki-Miyaura Coupling Reaction

Baocang Liu,^{a,b,c} Yuefang Niu,^a Yan Li,^a Fan Yang,^a Jiamin Guo,^a Qin Wang,^{a,c} Peng Jing,^a Jun Zhang,^{a,b,c} and Guohong Yun^c*

^aCollege of Chemistry and Chemical Engineering, Inner Mongolia University, Hohhot 010021, P. R. China.

^bCollege of Life Science, Inner Mongolia University, Hohhot 010021, P. R. China

^cInner Mongolia Key Lab of Nanoscience and Nanotechnology, Inner Mongolia University, Hohhot 010021, P. R. China

*Corresponding author: J. Zhang, Tel.: +86 471 4992175, Fax: +86 471 4992278, E-mail:

cejzhang@imu.edu.cn

Experimental Section

1. Materials

Tetraethyl orthosilicate (TEOS), tetrabutyl orthotitanate (TBOT), palladium (II) chloride (PdCl_2), cetyltrimethylammonium bromide (CTAB), and NaBH_4 (AR $\geq 98\%$) were purchased from Sinopharm Chemical Reagent Co., Ltd. Absolute ethanol, ammonia solution (25-28 wt %), and formaldehyde (37% solution) were obtained from Tianjin Windship Chemistry Technological Co., Ltd. Hydroxy propyl cellulose (HPC, MW = 80,000) and poly(vinyl alcohol) (PVA, Mw = 10,000) were obtained from Sigma-Aldrich. 3-Aminopropyl-triethoxysilane (APTES, 99%), 4-nitrophenol (AR), resorcinol (AR), and all reagents used in Suzuki–Miyaura coupling reaction were purchased from Aladdin. All chemicals were used as received without further treatment. Deionized water was used for all experiments.

2. Synthesis of nanocatalysts

2.1. Synthesis of @meso-TiO₂-NH₂ spheres

Monodisperse SiO₂ spheres were synthesized via a Stöber sol-gel method according to the previous report,¹ and were used as scarified templates for synthesis of @TiO₂ spheres. The synthesis of @TiO₂ spheres follows a previously reported method with a slight modification.² Typically, an aqueous solution containing SiO₂ spheres (5 mL) was dispersed in the mixture of hydroxypropyl cellulose (HPC, 0.4 g), distilled water (0.4 mL), and absolute ethanol (100 mL) under vigorous magnetic stirring for 30 min. TBOT (4 mL) previously dissolved in absolute ethanol (20 mL) was introduced dropwise at a rate of 0.5 mL/min. Afterward, the solution was refluxed at 85 °C for 100 min to obtain SiO₂@TiO₂ spheres. The SiO₂@TiO₂ spheres were separated and washed with ethanol for five times. Then, the SiO₂@TiO₂ spheres

were dispersed in NaOH aqueous solution (0.25 M, 40 mL) to remove SiO₂ cores to achieve the hollow meso-TiO₂ (@meso-TiO₂). The @meso-TiO₂ spheres were isolated by centrifugation and washed with deionized water and ethanol for several times. Finally, the @meso-TiO₂ spheres were re-dispersed in ethanol (10 mL) for further use. The @meso-TiO₂ sphere solution was dispersed into absolute ethanol (30 mL) and APTES (0.2 mL) was added and stirred at room temperature for 12 h to ensure the amino groups to be decorated on the surface of @meso-TiO₂ spheres. The white precipitates were collected by centrifugation and washed with ethanol, and then were re-dispersed in deionized water (10 mL).

2.2. Synthesis of @meso-TiO₂-NH₂/Pd²⁺ spheres

To the above @meso-TiO₂-NH₂ solution, 5 mL of PdCl₂ solution (1 g/L) was added and the mixture solution was diluted to 100 mL with deionized water. After stirring for 12 h, the products were collected by centrifugation and washed with deionized water for five times, and then were re-dispersed in ethanol (10 mL).

2.3. Synthesis of @meso-TiO₂/Pd spheres

The @meso-TiO₂/Pd spheres were prepared via a colloidal deposition method with some modification.³ In a typical procedure, PdCl₂ solution (1 g/L, 5 mL) and PVA solution (1 wt%, 0.36 mL) were diluted to 100 mL with deionized water under vigorous stirring. After 30 min, NaBH₄ solution (0.1 mol/L, 1.4 mL) was injected into the above solution, and a dark-brown solution was obtained, which indicated that the Pd colloids were formed. After another 30 min, 10 mL of @meso-TiO₂-NH₂ was added immediately. After stirring for 4 h, the Pd colloids were completely absorbed, as indicated by the discoloration of the solution. The @meso-TiO₂/Pd spheres were collected by centrifugation, and washed with deionized water

for five times to completely remove the chloride ion.

2.4. Synthesis of @Pd/meso-TiO₂/Pd@meso-SiO₂, @meso-TiO₂/Pd@meso-SiO₂, and @meso-TiO₂/Pd@SiO₂ spheres

To synthesize the @Pd/meso-TiO₂/Pd@meso-SiO₂, @meso-TiO₂/Pd@meso-SiO₂, and @meso-TiO₂/Pd@SiO₂ spheres, the @Pd²⁺/meso-TiO₂/Pd²⁺@RF and @meso-TiO₂/Pd@RF spheres were firstly synthesized via a polymerization described as follows.⁴ Typically, the above the @meso-TiO₂/Pd solution was added into a beaker charged with deionized water (50 mL), ammonia solution (0.18 mL), and CTAB (0.027g) under stirring for 30 min. Afterward, resorcinol (0.23 g) and formaldehyde solution (0.35 mL) were added, and the reaction was carried out at room temperature for 16 h under continuous magnetic stirring. The @meso-TiO₂/Pd²⁺@RF and @ Pd²⁺/meso-TiO₂/Pd@RF spheres were obtained by centrifugation and washed with deionized water and absolute ethanol for three times, respectively.

The @Pd/meso-TiO₂/Pd@meso-SiO₂, @meso-TiO₂/Pd@meso-SiO₂, and @meso-TiO₂/Pd@SiO₂ spheres were synthesized as follows: typically, the aqueous solution of @Pd²⁺/meso-TiO₂/Pd²⁺@RF and @meso-TiO₂/Pd@RF spheres (10 mL) were dispersed in a mixture of deionized water (60 mL), ethanol (100 mL), ammonia aqueous(1 mL), and CTAB (0.3 g) under vigorously magnetic stirring for 0.5 h. Then, TEOS (0.3 mL) was introduced and the reaction was maintained for 12 h at room temperature to obtain the @Pd²⁺/meso-TiO₂/Pd²⁺@RF@SiO₂ and @meso-TiO₂/Pd@RF@SiO₂, respectively. The @Pd²⁺/meso-TiO₂/Pd²⁺@RF@SiO₂ and @meso-TiO₂/Pd@RF@SiO₂ spheres were isolated by centrifugation, and washed with de-ionized water and ethanol, and dried in oven at 80 °C for 12 h. The @PdO/meso-TiO₂/PdO@meso-SiO₂ and @meso-TiO₂/PdO@meso-SiO₂ spheres

were obtained under calcination at 550 °C for 3 h. Then, the @PdO/meso-TiO₂/PdO@meso-SiO₂ and @meso-TiO₂/PdO@meso-SiO₂ spheres were reduced in a hydrogen atmosphere at 300 °C (14 % hydrogen and 86 % argon) for 2 h to obtain the final @Pd/meso-TiO₂/Pd@meso-SiO₂ and @meso-TiO₂/Pd@meso-SiO₂ spheres.

To synthesize the @Pd/meso-TiO₂/Pd@SiO₂ spheres, the above obtained @Pd²⁺/meso-TiO₂/Pd²⁺@RF solution was added into a beaker charged with absolute ethanol (66 mL), deionized water (4.2 mL), and ammonia solution (3.4 mL) under stirring for 30 min. Afterward, TEOS (0.4 mL) was added, and the reaction was carried out at room temperature for 24 h under continuous magnetic stirring. The @Pd²⁺/meso-TiO₂/Pd²⁺@RF@SiO₂ spheres were isolated by centrifugation, and washed with de-ionized water and ethanol, and then dried in an oven at 80 °C for 12 h. The @PdO/meso-TiO₂/PdO@SiO₂ spheres were obtained under calcination at 550 °C for 3 h. Then, the @PdO/meso-TiO₂/PdO@SiO₂ were reduced in a hydrogen atmosphere (14 % hydrogen and 86 % argon) at 300 °C for 2 h to obtain the final @Pd/meso-TiO₂/Pd@SiO₂ spheres.

2.5. Synthesis of @Pd/meso-TiO₂/Pd and @meso-TiO₂/Pd spheres

For comparison, the @Pd/meso-TiO₂/Pd and @meso-TiO₂/Pd spheres were synthesized via the calcination of @meso-TiO₂-NH₂/Pd²⁺ and @meso-TiO₂-NH₂/Pd spheres at 600 °C for 3 h following the reduction under H₂ atmosphere (14 % hydrogen and 86 % argon) at 300 °C for 2 h.

3. Characterization

Powder X-ray diffraction (XRD) and Small Angle Powder X-ray diffraction (SAXRD) were performed using a PANalytical Empyrean diffractometer. Scanning transmission electron

microscopy (STEM) and transmission electron microscopy (TEM) characterization was performed on a FEI tacnai F20 field-emission transmission electron microscope (FE-TEM). Scanning electron micrographs were recorded with a HITACHI S4800 field-emission scanning electron microscope (FE-SEM). The absorption spectra were recorded using a SPECORD.50 UV-vis spectrophotometer (Analytikjena). Fourier transform infrared spectroscopy (FT-IR) was performed on MAGNA-IR750 spectrometer by using KBr pellets. Surface area measurements were performed on an ASAP 2010 Brunauer-Emmett-Teller (BET) analyzer. Actual Pd content in the nanocatalysts was estimated with a VARIAN VISTA-MPX ICP-Mass spectroscopy (MS, USA).

4. Catalytic tests

The Suzuki–Miyaura coupling reaction of aryl iodides and phenylboronic acid was carried out in a sealed heavy wall pressure vessel (35 mL). All reactions and manipulations were run under air atmosphere. Typically, a reaction tube was charged with aryl iodide (0.5 mmol), aryl boronic acid (1 mmol), catalyst (20 mg), K_2CO_3 (1 mmol), and absolute ethanol (10 mL). The mixture was stirred at 80 °C, and monitored by HPLC at specific time. The crude product was characterized by HPLC analysis (HITACHI, D 2000 with a 25 cm Lachrom C18 column and UV-visible detector with measurement wavelength at 254 nm)

The catalytic performance for reduction of 4-nitrophenol to 4-aminophenol with $NaBH_4$ aqueous solution at room temperature was carried out as follows: Typically, the catalyst (2 mg) was added into millipore water (40 mL) to form a homogeneous suspension by ultrasonication. Then, $NaBH_4$ aqueous solution (0.5 M, 0.5 mL) was added into the above suspension, and the suspension was stirred at room temperature for 10 min. Then, 4-

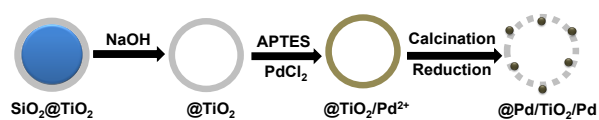
nitrophenol (0.012 M, 0.25 mL) was infused into the above suspension. After stirring several seconds, the mixture was rapidly transferred to the quartz cell to monitor the reaction progress by measuring the UV-vis absorption spectra of the mixture to evaluate the catalytic activity and stability of the catalysts, as the reactant of 4-nitrophenol has a strong absorption peak at 400 nm, while the product of 4-aminophenol has a median absorption peak at 295 nm.

5. Catalytic performance of “shell-in-shell” @Pd/meso-TiO₂/Pd@meso-SiO₂ catalyst for 4-nitrophenol reduction reaction

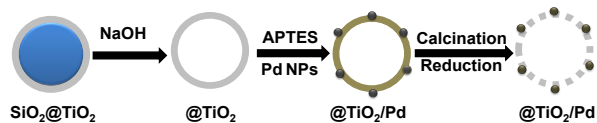
The catalytic performance of @Pd/meso-TiO₂/Pd@meso-SiO₂ and @meso-TiO₂/Pd@meso-SiO₂ nanocatalysts were also evaluated using model reaction of the reduction of 4-nitrophenol (4-NP) to 4-aminophenol (4-AP) with NaBH₄ aqueous solution at room temperature. The evolution of UV-vis spectra with reaction time for the reduction of 4-NP to 4-AP on different catalysts is monitored (Fig. S13a and b). It shows that the @Pd/meso-TiO₂/Pd@meso-SiO₂ catalyst possesses superior catalytic activity to @meso-TiO₂/Pd@meso-SiO₂ nanocatalyst, and the complete conversion of 4-NP to 4-AP can be realized within 10 min. The reduction rates shown in Fig. S13c indicate that @Pd/meso-TiO₂/Pd@meso-SiO₂ and @meso-TiO₂/Pd@meso-SiO₂ nanocatalysts exhibit excellent catalytic performance and that 4-NP can be completely reduced to 4-AP within 14 min. The linear fit with a coefficient of determination very close to unity also supports the assumption of pseudo-first-order kinetics (Fig. S13d) according to a linear relation of $\ln(C_t/C_0)$ versus reaction time.⁵ The @Pd/meso-TiO₂/Pd@meso-SiO₂ catalyst shows the fastest reaction rate in comparison with others, and the apparent kinetic rate constant is estimated to be 0.34 min⁻¹. The catalytic reusability test shows that the catalytic activity almost maintain constant even after ten cycles running (Fig.

S13e and f), suggesting the outstanding catalytic stability of the nanocatalyst. The catalytic performance tests implies that the “shell-in-shell” @meso-TiO₂/Pd@meso-SiO₂ nanocatalyst can be used as a nanoreactor for efficient catalysis of various reactions, and its high catalytic activity may largely rely on the novel design of “shell-in-shell” structural configuration with merits for improving the catalytic performance.

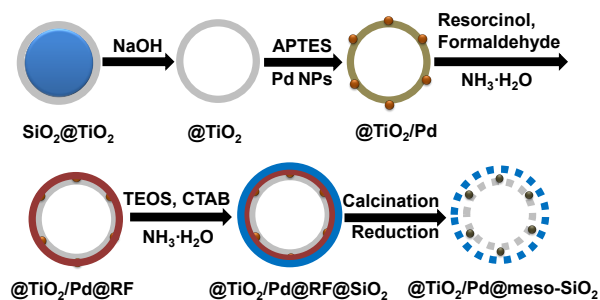
Route I



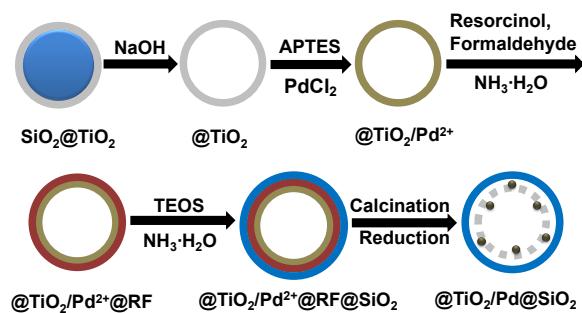
Route II



Route III

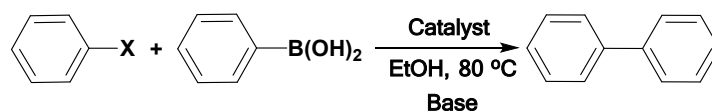


Route IV



Scheme S1. Schematic illustration for synthesis of different nanocatalysts. Route I: single-shell $@\text{Pd}/\text{meso-TiO}_2/\text{Pd}$ spheres, Route II: single-shell $@\text{meso-TiO}_2/\text{Pd}$ spheres, Route III: “shell-in-shell” $@\text{meso-TiO}_2/\text{Pd}@meso\text{-SiO}_2$ spheres, and IV: “shell-in-shell” $@\text{meso-TiO}_2/\text{Pd}@SiO_2$ spheres.

Table S1 Suzuki–Miyaura coupling reactions of aryl halides and phenylboronic acid over different catalysts^a



^a Reaction conditions: 80 °C, ethanol (10 mL), iodobenzene (0.5 mmol), phenylboronic acid (1 mmol), K₂CO₃ or Cs₂CO₃ (1 mmol), catalyst (10 mg or 25 mg), reaction time (0.5h).

^b Determined by HPLC using pentamethylbenzene as internal standard.

Nanocatalysts	X	Base	Cat./mg	Pd/wt.%	Time/min	Con./% ^b	TOF/h ^{-1c}
@Pd/meso-TiO ₂ /Pd@meso-SiO ₂	I	K ₂ CO ₃	10	0.21	30	99	5130
@meso-TiO ₂ /Pd@meso-SiO ₂	I	K ₂ CO ₃	20	0.20	20	98	3961
@Pd/meso-TiO ₂ /Pd	I	K ₂ CO ₃	10	0.30	30	99	3476
@meso-TiO ₂ /Pd	I	K ₂ CO ₃	20	0.48	20	99	1632
@Pd/meso-TiO ₂ /Pd@SiO ₂	I	K ₂ CO ₃	10	0.17	30	2	124
@Pd/meso-TiO ₂ /Pd @meso-SiO ₂	Br	Cs ₂ CO ₃	25	0.21	60	99	1026
@meso-TiO ₂ /Pd@meso-SiO ₂	Br	Cs ₂ CO ₃	25	0.20	60	90	960
@Pd/meso-TiO ₂ /Pd	Br	Cs ₂ CO ₃	30	0.30	60	88	515
@meso-TiO ₂ /Pd	Br	Cs ₂ CO ₃	30	0.48	60	83	304
@Pd/meso-TiO ₂ /Pd@SiO ₂	Br	Cs ₂ CO ₃	25	0.17	60	3	37

^c TOF is calculated by moles of product per molar Pd per hour.

Table S2 The catalytic performance of mesoporous “shell-in-shell” @Pd/meso-TiO₂/Pd@meso-SiO₂ nanocatalyst for Suzuki–Miyaura coupling reaction at different temperatures.^a

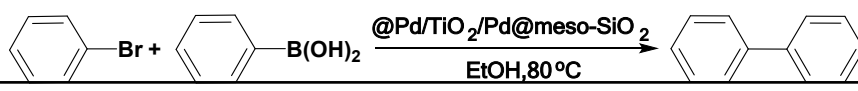


Temperature /°C	X	Cat./mg	Time/min	Con./% ^b
50	I	10	30	67
60	I	10	30	87
70	I	10	30	98
80	I	10	30	99
40	Br	25	240	33
50	Br	25	240	54
60	Br	25	240	72
70	Br	25	240	97
80	Br	25	240	99

^a Reaction conditions: 80 °C, ethanol (10 mL), iodobenzene (0.5 mmol), phenylboronic acid (1 mmol), K₂CO₃ or Cs₂CO₃ (1 mmol), catalyst (10 mg or 25 mg), reaction time (0.5h).

^b Determined by HPLC using pentamethylbenzene as internal standard.

Table S3 The catalytic performance of mesoporous “shell-in-shell” @Pd/meso-TiO₂/Pd@meso-SiO₂ nanocatalyst for Suzuki–Miyaura coupling reaction under the condition of different alkali.^a

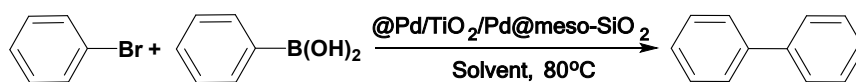


Base	Cat./mg	T/min	Con./% ^b
Cs ₂ CO ₃	25	60	99
K ₂ CO ₃	25	240	99
CH ₃ ONa	25	240	99
Na ₂ CO ₃	25	240	98
NaHCO ₃	25	240	96
KOH	25	240	8
NaOH	25	240	6
LiOH	25	240	4
triethylamine	25	240	10

^a Reaction conditions: ethanol (10 mL), iodobenzene (0.5 mmol), phenylboronic acid (1 mmol).

^b Determined by HPLC using pentamethylbenzene as internal standard.

Table S4 The catalytic performance of mesoporous “shell-in-shell” hollow @Pd/TiO₂/Pd@meso-SiO₂ nanocatalyst for Suzuki–Miyaura coupling reactions in different solvent.^a



Solvent	Cat./mg	Time/min	Con./% ^b
EtOH	25	240	99
DMF	25	240	11
Toluene	25	240	9
DMSO	25	240	8
CH ₃ CN	25	240	12
cyclohexane	25	240	6
dioxane	25	240	13

^a Reaction conditions: ethanol (10 mL), iodobenzene (0.5 mmol), phenylboronic acid (1 mmol).

^b Determined by HPLC using pentamethylbenzene as internal standard.

Table S5 The leaching content of Pd for “shell-in-shell” @Pd/meso-TiO₂/Pd@meso-SiO₂ and Pd/SiO₂ (SOL-IMP) catalysts before and after one cycle catalytic testing as determined by ICP-MS measurement.

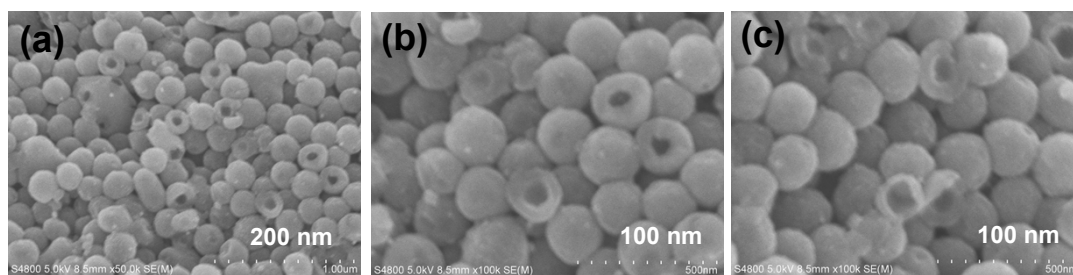
Pd content	Before testing	After one cycle testing
Pd content in @Pd/meso-SiO ₂ /Pd@meso-SiO ₂ catalyst	0.21 wt %	0.20 wt %
Pd content in mother liquor	0 µg·mL ⁻¹	0.06 µg·mL ⁻¹
Pd content in Pd/SiO ₂ (SOL-IMP) catalyst	0.98 wt %	0.92 wt %
Pd content in mother liquor	0 µg·mL ⁻¹	0.31 µg·mL ⁻¹

^a Reaction conditions: 80 °C, ethanol (10 mL), bromobenzene (0.5 mmol), phenylboronic acid (1 mmol), Cs₂CO₃ (1 mmol), reaction time: 60 min.

^b Determined by HPLC using pentamethylbenzene as internal standard.

Table S6. Suzuki–Miyaura coupling reaction of bromobenzene and phenylboronic acid in the mother liquor after one cycle catalytic testing and over its corresponding @Pd/meso-SiO₂/Pd@meso-SiO₂ catalyst^a.

Nanocatalysts	Base	Cat./mg	Time/min	Con./% ^b
Mother liquor after one cycle catalytic testing	Cs ₂ CO ₃	-	60	<1
@Pd/meso-SiO ₂ /Pd@meso-SiO ₂ (Recycled)	Cs ₂ CO ₃	23	60	98



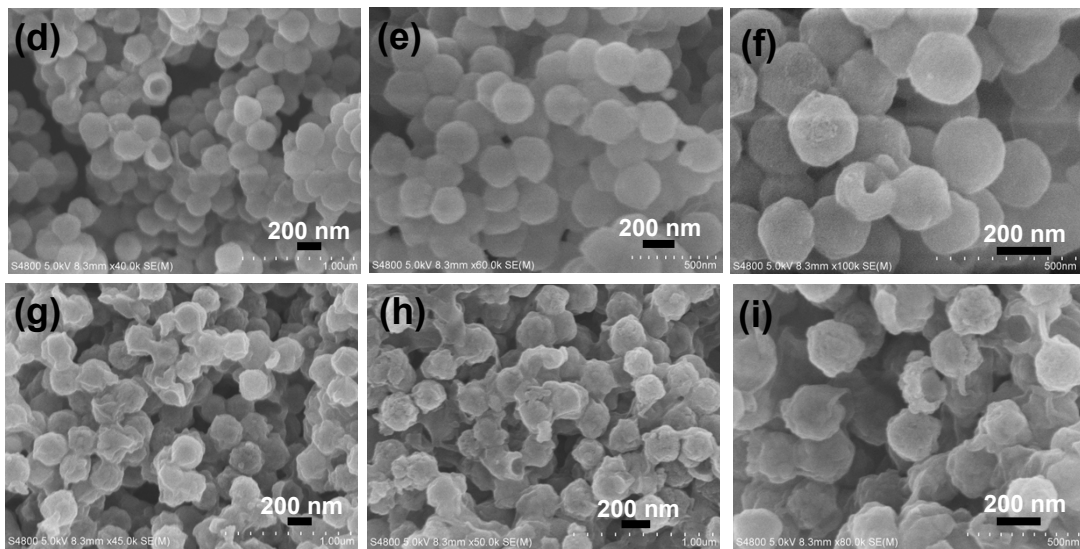
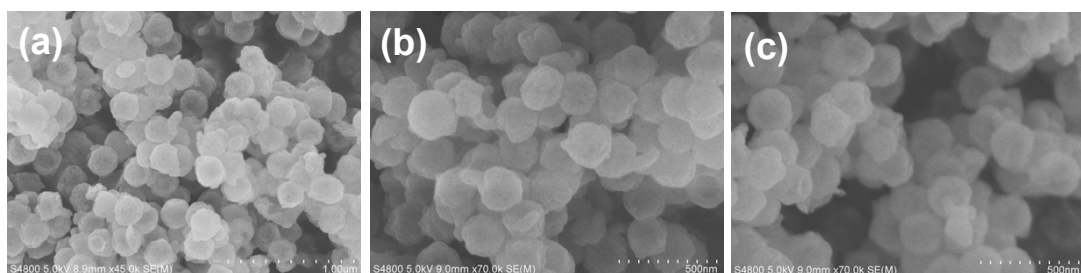


Fig. S1 SEM images of (a-c) single-shell @Pd²⁺/meso-TiO₂/Pd²⁺ spheres, (d-f) “shell-in-shell” @Pd²⁺/meso-TiO₂/Pd²⁺@RF spheres, and (g-i) triple-shell @Pd²⁺/meso-TiO₂/Pd²⁺@RF@meso-SiO₂ spheres.



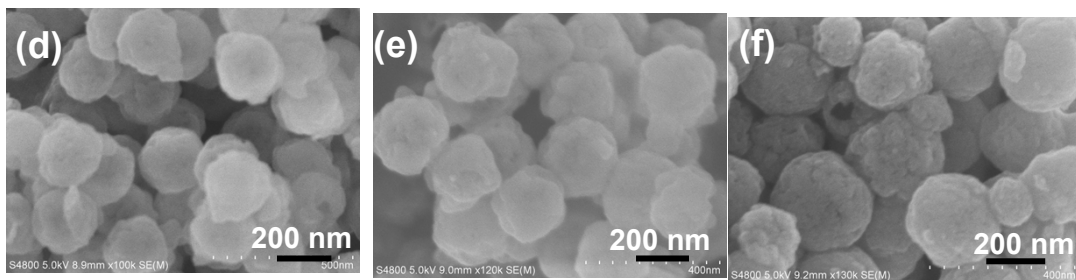
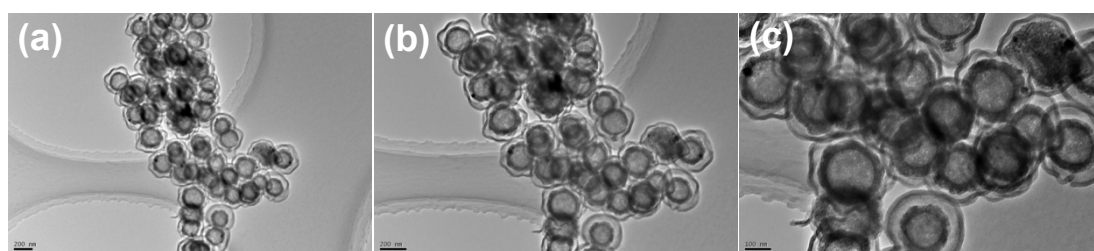


Fig. S2 (a-f) SEM images of mesoporous "shell-in-shell" $@Pd/meso-TiO_2/Pd@meso-SiO_2$ nanocatalyst.



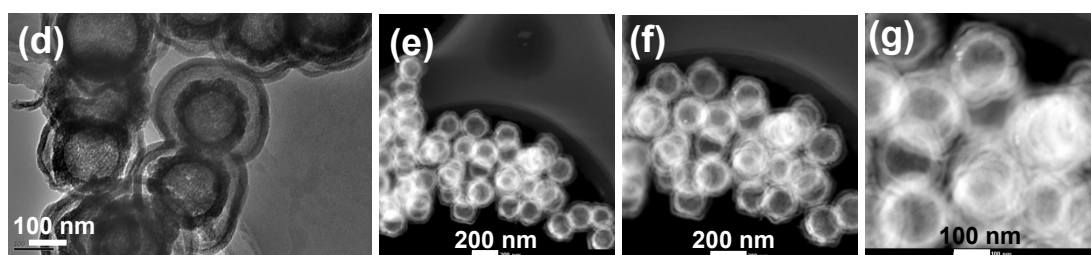
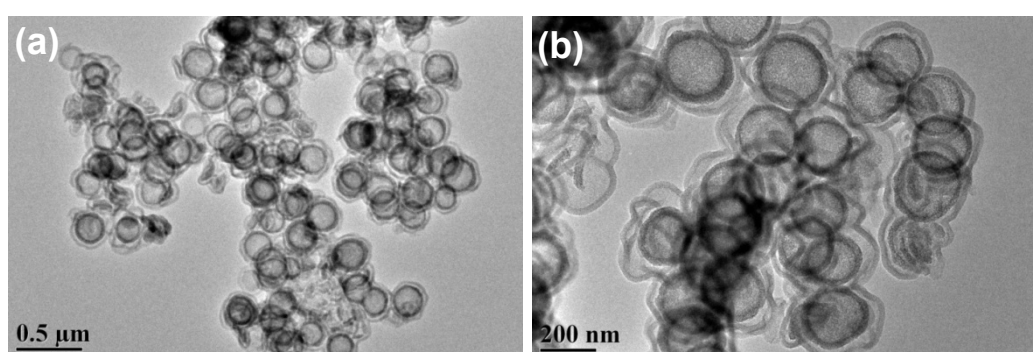


Fig. S3 TEM (a-d) and STEM images (e-g) of mesoporous "shell-in-shell" structured $@Pd/meso-TiO_2/Pd@meso-SiO_2$ nanocatalyst.



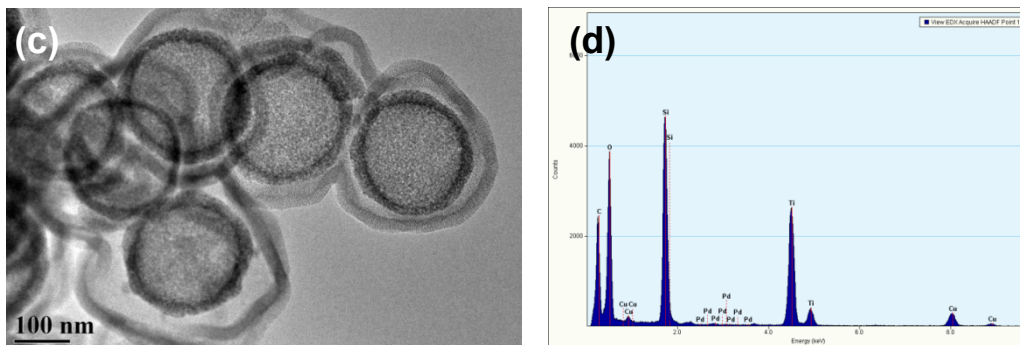


Fig. S4 TEM images (a-c) and EDX spectrum (d) of mesoporous “shell-in-shell” structured @Pd/meso-TiO₂/Pd@meso-SiO₂ nanocatalyst.

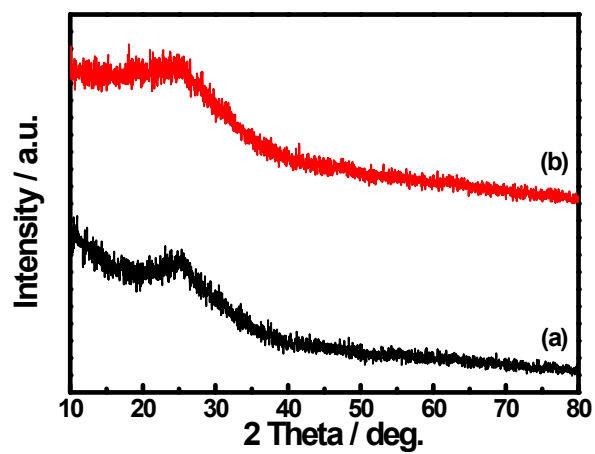


Fig. S5 XRD patterns of (a) @Pd/meso-TiO₂/Pd@meso-SiO₂ and (b) @ meso-TiO₂/Pd²⁺@RF@SiO₂ nanocatalysts.

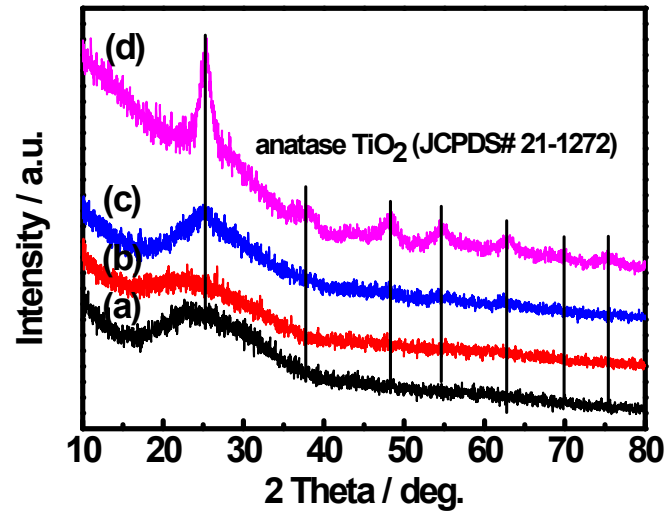


Fig. S6 XRD patterns of @Pd/meso-TiO₂/Pd@meso-SiO₂ sphere calcinated at (a) 450 °C, (b) 550 °C, (c) 650°C, and (d) 750 °C.

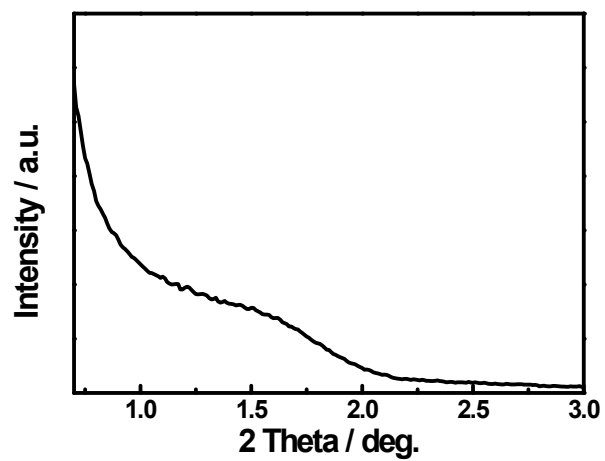


Fig. S7 SAXRD of mesoporous “shell-in-shell” @Pd/meso-TiO₂/Pd@meso-SiO₂ nanocatalyst.

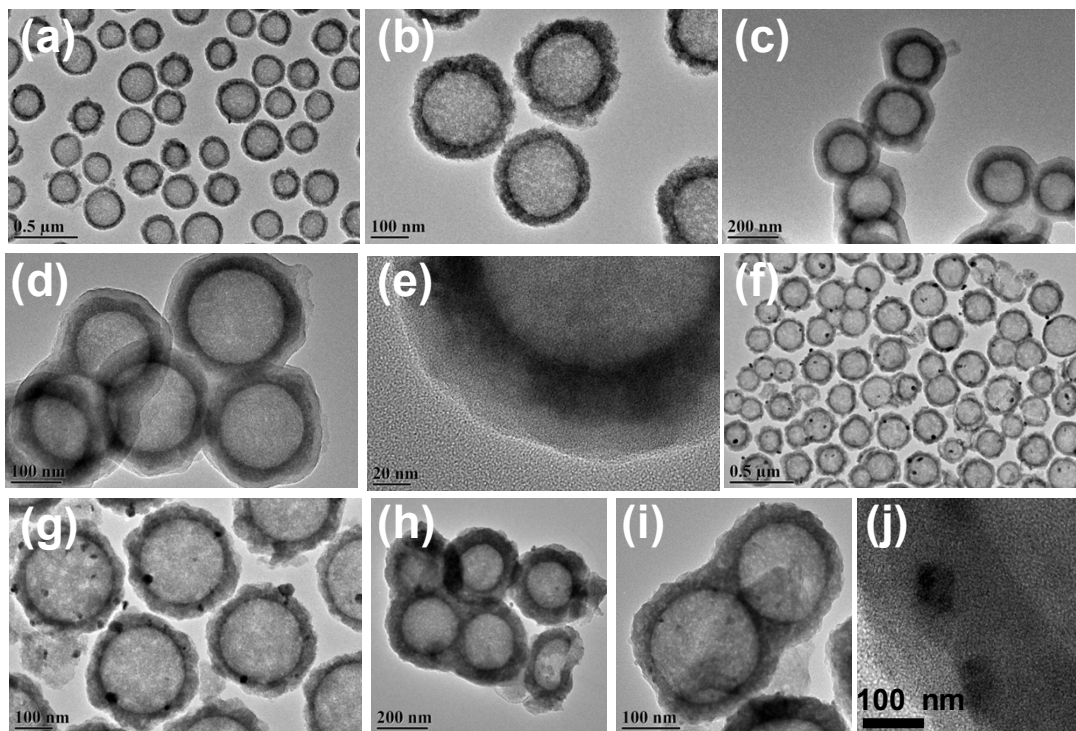


Fig. S8 TEM images of (a and b) @meso-TiO₂/Pd²⁺ spheres, (c-e) @ meso-TiO₂/Pd²⁺@RF spheres, (f and g) @Pd/meso-TiO₂/Pd spheres, and (h-j) @meso-TiO₂/Pd spheres.

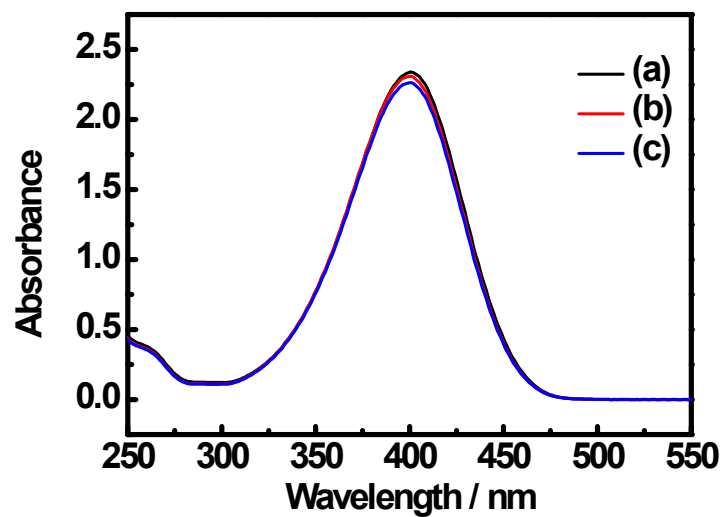


Fig. S9 The absorbance change of the 4-nitrophenol solution after 30 min absorption: (a) the original 4-nitrophenol solution, (b) the solution with traditional Pd/SiO₂ catalyst, and (c) the solution with “shell-in-shell” @Pd/meso-SiO₂/Pd@meso-TiO₂ catalyst.

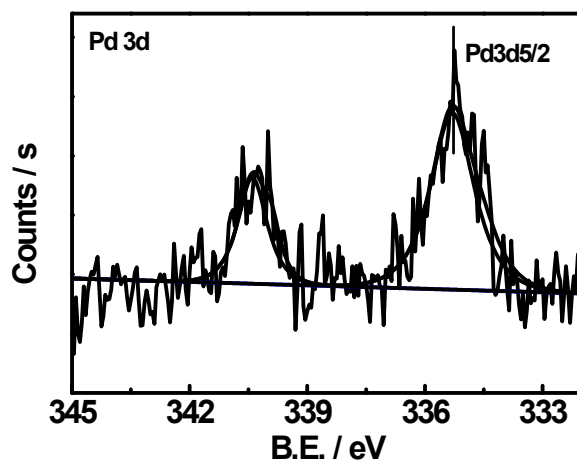


Fig. S10 Experimental and fitted XPS spectra of Pd3d of mesoporous “shell-in-shell” hollow @Pd/meso-TiO₂/Pd@meso-SiO₂ nanocatalyst.

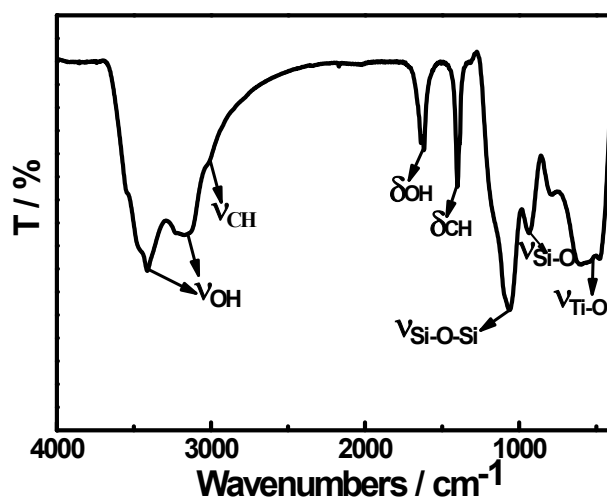


Fig. S11 FT-IR spectrum of mesoporous "shell-in-shell" @Pd/meso-TiO₂/Pd@meso-SiO₂ nanocatalyst.

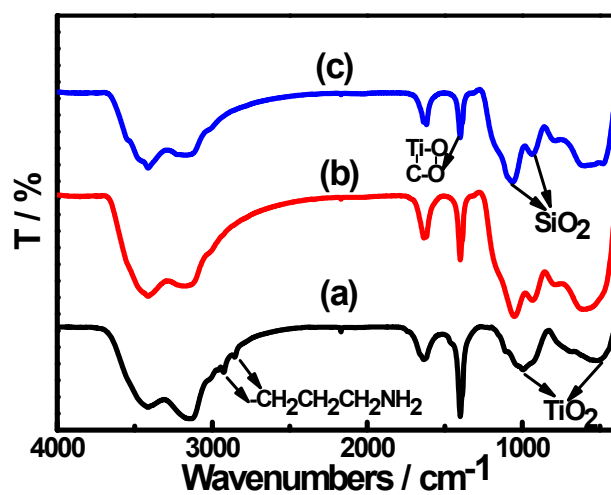


Fig. S12 FT-IR spectra of (a) @meso-TiO₂-NH₂/Pd²⁺, (b) @meso-TiO₂/Pd@meso-SiO₂, and (c) @Pd/meso-TiO₂/Pd@meso-SiO₂ nancatalysts.

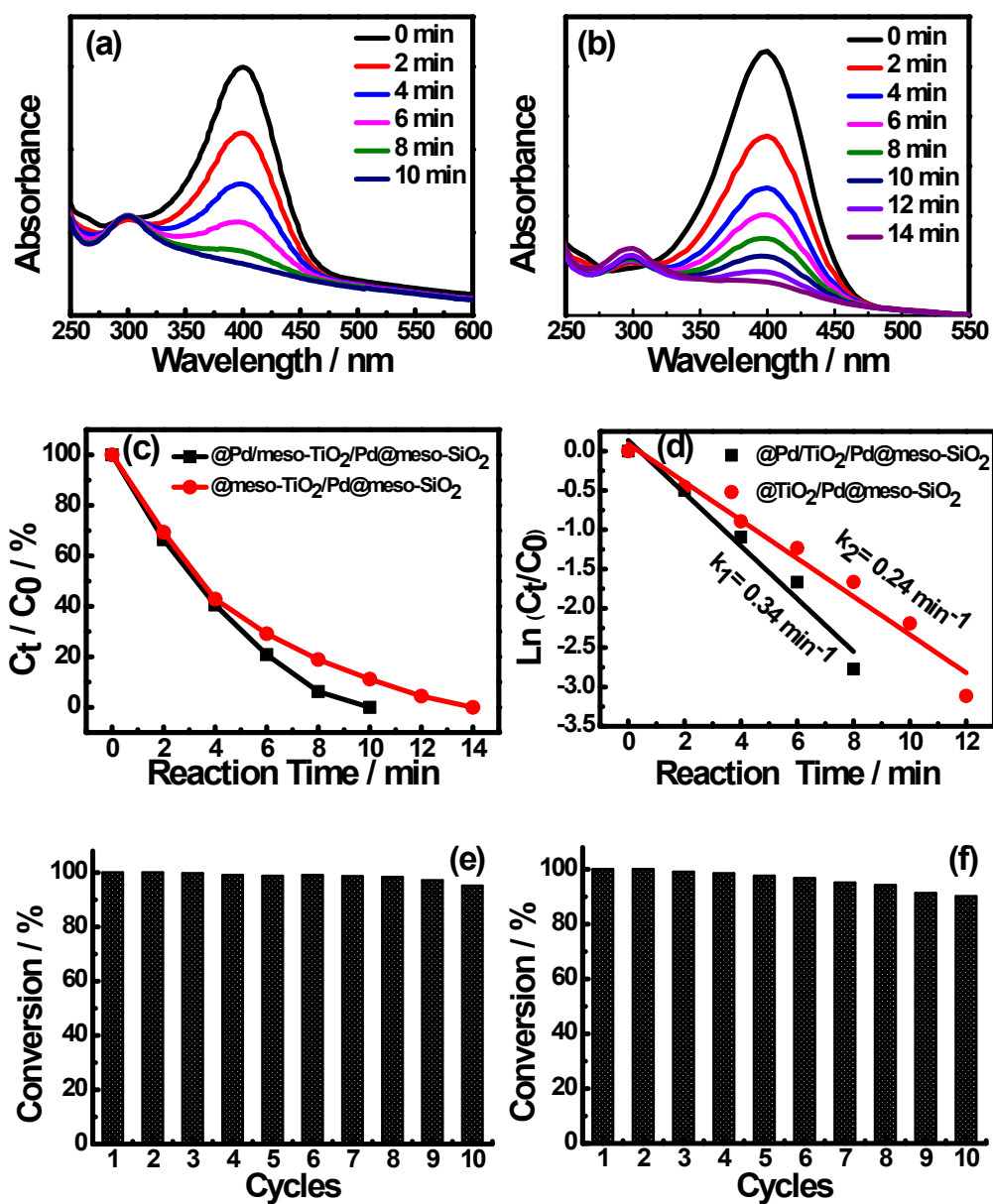


Fig. S13 (a and b) UV-vis spectra showing the reduction of 4-NP to 4-AP on $@Pd/meso-TiO_2/Pd@meso-SiO_2$ and $@meso-TiO_2/Pd@meso-SiO_2$ nanocatalysts, (c) Catalytic tests of the reduction rate for the reduction of 4-NP on $@Pd/meso-TiO_2/Pd@meso-SiO_2$ and $@meso-TiO_2/Pd@meso-SiO_2$ nanocatalysts; (d) Plot of $\ln(C_t/C_0)$ against the reaction time of $@Pd/meso-TiO_2/Pd@meso-SiO_2$ and $@meso-TiO_2/Pd@meso-SiO_2$ nanocatalysts; and (e and f) Catalytic stability tests of $@Pd/meso-TiO_2/Pd@meso-SiO_2$ and $@meso-TiO_2/Pd@meso-SiO_2$ nanocatalysts.

References

1. N. C. Strandwitz, S. Shaner, and G. D. Stucky, *J. Mater. Chem.*, 2011, **21**, 10672-10675.
2. J. B. Joo, Q. Zhang, M. Dahl, I. Lee, J. Goebel, F. Zaera and Y. D. Yin, *Energ. Environ. Sci.*, 2012, **5**, 6321-6327.
3. L. Kesavan, R. Tiruvalam, M. H. Ab Rahim, M. I. bin Saiman, D. I. Enache, R. L. Jenkins, N. Dimitratos, J. A. Lopez-Sanchez, S. H. Taylor, D. W. Knight, C. J. Kiely and G. J. Hutchings, *Science*, 2011, **331**, 195-199.
4. N. Li, Q. Zhang, J. Liu, J. Joo, A. Lee, Y. Gan and Y. Yin, *Chem. Commun.*, 2013, **49**, 5135-5137.
5. M. Pérez-Lorenzo, B. Vaz, V. Salgueiriño and M. A. Correa-Duarte, *Chem -A. Eur. J.*, 2013, **19**, 12196-12211.